Range-based Radar Model Structure Selection

Andreas Jansson[†*], Filip Elvander[*], Peter Almers[†], and Andreas Jakobsson[*]
[*]Division of Mathematical Statistics, Lund University, Sweden
[†]Acconeer AB, Scheelevägen 27, Lund, Sweden

***Abstract*—In this work, we study under which circumstances it is appropriate to use simplified models for range determination using radar. Typically, pulsed radar systems result in the backscattered, demodulated, and matched signal having a chirp signal structure, with the frequency rate being related to the range to the reflecting target and the relative velocity of the transmitter and reflector. Far from the target, and at low relative velocities, one may achieve preferable location estimates by neglecting the frequency rate, treating the received signal as being purely sinusoidal, whereas at close range, neglecting the frequency rate notably reduces the achievable performance. Using misspecified estimation theory, we derive a lower bound of the achievable performance when neglecting the true signal structure, and show at which ranges one model is preferable to the other. Numerical results from a mm-wave radar system illustrate the results.**

***Index Terms*—Range estimation, Radar systems, Misspecified Cramér-Rao lower bound**

I. Introduction

Radar research and technology has a long and illustrious history, and has for decades been used on an everyday basis in a wide range of applications, ranging from classical problem such as air surveillance to more recent topics such as fall prevention and close-range surface identification [1]–[8]. Radar systems have several attractive properties relevant for these application areas, such as a high tolerance for environmental influences like weather and lighting conditions, as well as allowing for accurate and fast identification of reflecting targets [8]. The technology initially gained notable interest in the 1930s prior to the Second World War, with significant progress then made during the war, which played a key part in deciding the victor [1].

Although the area has attracted substantial interest since, it is still a highly active area of research. One recent trend has been the development of small and energy efficient mm-wave radars such as Acconeer's A1 radar sensor [7], [8] and Google's Project Soli [9]. Such small-scale pulsed radars can be employed in a variety of close range applications, such as gesture control [10], surface identification [8], and object detection [11]. Generally, this form of pulsed systems transmit a rapid succession of sinusoidal pulses, whereafter the received backscatters are demodulated and matched with the transmitted signal in order to determine the distance to the reflecting object [3], [4]. In cases when the radar and the reflector move relative to one another, the resulting signal may generally be well modeled as a linear chirp signal, with the frequency rate being related to the relative motion and distance to the reflecting object [12], [13]. At large distances, relative to the pulse frequency, the resulting chirp rate is typically close to negligible, but as the object gets closer to the transmitter, the frequency rate becomes significant, and will yield reduced performance if ignored. In order to efficiently process the received signal, one should therefore use a parametric model incorporating the chirp rate in cases when one is close to the reflector, whereas it may be beneficial both from a computational and performance perspective to neglect this signal structure when the reflector is further from the transmitter.

In this work, we examine a theoretical framework for determining under which circumstances, and in particular at what transmitter-reflector range, it is beneficial to take the chirp rate into account when estimating the target location, and when one actually achieves better performance by neglecting this structure. By comparing a lower bound on the achievable estimation performance when taking the chirp rate into account, as given by the Cramér-Rao lower bound (CRLB) (see, e.g., [14]), with that of the misspecified CRLB (MCRLB) [15]–[18] resulting from neglecting the actual chirp structure and instead, assuming that the signal is only constructed from a sinusoidal reflection, we determine the range at which one of the model is preferable to the other. The work is related to recent efforts examining how a system's performance is affected by incorrectly assuming an signal structure that differs from the actual signal's [19], [20]. Using the resulting MCRLB for the considered radar problem, we determine at which distance the simplistic model actually allows for a preferable performance as compared to the signal's actual structure. Numerical results illustrate the results from a close-range mm-wave radar system, although it should be stressed that the results are general and are applicable to other settings as well.

II. Signal model

In this work, we consider the pulsed radar system shown in Figure 1, consisting of a transmitter-sensor system moving in relation to the reflecting object. For notational simplicity, we will assume that the target is stationary whereas the sensor is moving with a constant known speed v_0, although it should be noted that the presented results directly generalize to the case when also the target is moving and/or the relative velocity varies over time. While moving, the pulsed radar transmits a time-limited sinusoidal pulse which reflects on the target, and when received by the sensor is matched with the transmitted

This work was partially supported by the Wallenberg AI, Autonomous Systems and Software Program (WASP) funded by the Knut and Alice Wallenberg Foundation.

pulse [3]. As the sensor moves, the resulting slow-time signal will yield a signal x_t, with wavelength

$$\tilde{\lambda}_t = \frac{\lambda}{2\cos\psi_t},$$

where λ and ψ_t denote the carrier wavelength (in meters) and the angle to the target, at time t, respectively. Thus, as the sensor approaches the target, the angle ψ_t will increase, thereby causing the wavelength $\tilde{\lambda}_t$ to also increase, as illustrated in Figure 1. The resulting signal may be well modeled as [3]

$$x_t = \alpha e^{i\int_0^t \varphi_\tau d\tau + i\phi}, \tag{1}$$

for $t = 0, 1, \ldots, N-1$, with $N \in \mathbb{N}$, where $\alpha > 0$, φ_t, and $\phi \in [-\pi, \pi)$ denote the amplitude, the instantaneous angular frequency, and initial phase, respectively. Specifically, assuming a linear chirp,

$$\varphi_t = \omega + rt, \tag{2}$$

with $\omega \in [-\pi, \pi)$ and $r \in \mathbb{R}$ denoting the initial frequency and chirp rate, respectively. In the discussed radar localization problem, the angular direction, ψ_t, of the target is related to the parameters of the chirp signal according to

$$\psi_t = g(\varphi_t) = g(\omega + rt),$$

where

$$g(\omega) = 180\pi^{-1}\arccos\left(\omega\frac{f_s\lambda}{4\pi v_0}\right)$$

with f_s and v_0 denoting the sampling frequency (in Hz) and the speed of the sensor (in m/s), respectively. Furthermore, the chirp rate r in (2) is related to ψ_t as well as the distance d to the target by

$$r = -\frac{4\pi v_0^2 \sin^2\psi_t}{\lambda d f_s^2}. \tag{3}$$

Under the assumption that $v_0 > 0$, the chirp rate is thus non-zero if and only if $\psi_t \notin \{0, \pi\}$ and d is finite. Herein, we are interested in determining the angular location of the target at the end of the measurement period, i.e.,

$$\psi_{N-1} = g(\varphi_{N-1}),$$

given a set of noisy measurements of x_t. Specifically, we seek to compute estimates

$$\hat{\psi}_{N-1} = g(\hat{\varphi}_{N-1}),$$

where $\hat{\varphi}$ is parametrized by finite-sample estimates of $\hat{\omega}$ and $\hat{r}$ based on the measurements

$$y_t = x_t + e_t,$$

for $t = 0, 1, \ldots, N-1$. In this work, we assume that e_t may be well modeled as a circularly symmetric white Gaussian noise with variance σ^2. Typically, in many practical estimation scenarios, $|r| \ll 1$, implying that

$$\varphi_{N-1} = \omega + r(N-1) \approx \omega.$$

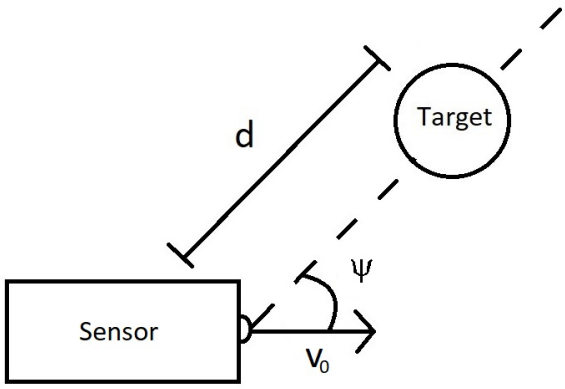

Fig. 1. The considered pulsed radar system.

This implies that a relevant question is whether a simplified sinusoidal waveform can be used in lieu of (1), possibly allowing for higher-accuracy estimates of ψ_{N-1}. That is, if one assumes the signal waveform

$$\mu_t = \alpha_0 e^{i\omega_0 t + i\phi_0}, \tag{4}$$

in place of (1), and computes an estimate of ψ_{N-1} as $g(\hat{\omega}_0)$ based on the sample vector $\mathbf{y}$ defined as

$$\mathbf{y} = \begin{bmatrix} y_0 & y_1 & \cdots & y_{N-1} \end{bmatrix}^T$$

what is the obtainable mean squared error (MSE) of $g(\hat{\omega}_0)$ as compared to $g(\hat{\varphi}_{N-1})$? In particular, as (4) contains fewer non-linear parameters than (1), it may even allow for more preferable estimates than taking the true signal model into account. In order to analyze this, one requires a useful definition of ω_0 when measurements are generated from the chirp model in (1), as well as finding a relevant bound on the variance of estimators of ω_0. Herein, we propose to address this using the framework of misspecified estimation.

III. Misspecified estimation

As to analyze the behavior of sinusoidal approximations of noisy measurements of the chirp signal in (1), one requires a definition of the frequency of (1), despite such a concept not existing in a strict physical sense. To this end, we propose to define the frequency ω_0 of (1) as the pseudo-true parameter [17] of the sinusoidal model in (4). Specifically, letting p_x denote the probability density function (pdf) of the signal measurement $\mathbf{y}$, where the subscript indicates the dependence on the chirp waveform, and letting p_μ denote the pdf of the sinusoidal approximation, the pseudo-true parameter

$$\boldsymbol{\theta}_0 = \begin{bmatrix} \alpha_0 & \phi_0 & \omega_0 \end{bmatrix}^T$$

is defined as

$$\boldsymbol{\theta}_0 = \arg\min_{\boldsymbol{\theta}} \; -\mathbb{E}_{p_x}\left(\log p_\mu(\mathbf{y};\boldsymbol{\theta})\right), \tag{5}$$

where $\mathbb{E}_{p_x}(\cdot)$ denotes the expectation with respect to p_x. That is, the pseudo-true parameter $\boldsymbol{\theta}_0$ minimizes the Kullback-Leibler divergence between the actual and assumed distributions of the signal. For the special case in which both p_x and

p_μ correspond to models with white Gaussian measurement noise, $\boldsymbol{\theta}_0$ can be computed as the parameter corresponding to the best ℓ_2 approximation of the actual signal waveform, i.e.,

$$\boldsymbol{\theta}_0 = \arg\min_{\boldsymbol{\theta}} \frac{1}{N}\sum_{t=0}^{N-1} |x_t - \mu_t(\boldsymbol{\theta})|^2 .$$

For the case considered herein, this implies that the pseudo-true frequency ω_0 can be found as

$$\omega_0 = \arg\max_{\omega} \Phi_x(\omega), \tag{6}$$

where Φ_x is the periodogram of the chirp waveform x_t, i.e.,

$$\Phi_x(\omega) = \frac{1}{N}\left|\sum_{t=1}^{N} x_t e^{-i\omega t}\right|^2 .$$

When both the chirp rate, r, and sample length, N, are small, the global maximum of Φ_x is unique, and the pseudo-true frequency, as given by (6), is given in closed form as

$$\omega_0 = \omega + \frac{N-1}{2}r = \varphi_{N-1} - \frac{N-1}{2}r.$$

Using (5) as the definition of the parameters of a sinusoidal approximation of (1) has a useful practical implication: under the assumption of uniqueness of $\boldsymbol{\theta}_0$, which holds for small enough (r, N), the misspecified maximum likelihood estimator (MMLE), i.e., the MLE derived under p_μ but applied to measurements from p_x, converges almost surely to $\boldsymbol{\theta}_0$ as the signal to noise ratio (SNR) tends to infinity [17]. As the periodogram estimate is the MLE for the sinusoidal signal, this implies that

$$\arg\max_{\omega} \Phi_y(\omega) \overset{a.s.}{\to} \omega_0,$$

as the noise variance $\sigma^2 \to 0$, where Φ_y denotes the periodogram of the noisy measurements y_t. Furthermore, a bound on the finite-sample variance of this estimate may be found as the MCRLB [16], [17]. Specifically, it can be shown that for any estimator $\hat{\boldsymbol{\theta}}_0$ of $\boldsymbol{\theta}_0$ that is unbiased under p_x, (see, e.g., [16], [19])

$$\mathbb{E}_{p_x}\left((\hat{\boldsymbol{\theta}} - \boldsymbol{\theta}_0)(\hat{\boldsymbol{\theta}} - \boldsymbol{\theta}_0)^T\right) \succeq A(\boldsymbol{\theta}_0)^{-1} F(\boldsymbol{\theta}_0) A(\boldsymbol{\theta}_0)^{-1} \tag{7}$$

where

$$A(\boldsymbol{\theta}_0) = \mathbb{E}_{p_x}\left[\nabla^2_{\boldsymbol{\theta}} p_\mu(\mathbf{y};\boldsymbol{\theta})\right]\Big|_{\boldsymbol{\theta}=\boldsymbol{\theta}_0} \tag{8}$$

$$F(\boldsymbol{\theta}_0) = \mathbb{E}_{p_x}\left[\nabla_{\boldsymbol{\theta}} p_\mu(\mathbf{y};\boldsymbol{\theta}) \nabla_{\boldsymbol{\theta}} p_\mu(\mathbf{y};\boldsymbol{\theta})^T\right]\Big|_{\boldsymbol{\theta}=\boldsymbol{\theta}_0}. \tag{9}$$

It may be noted that for the special case when $p_x = p_\mu$, for some $\boldsymbol{\theta}_0$, $F(\boldsymbol{\theta}_0) = -A(\boldsymbol{\theta}_0)$ is the Fisher information matrix, and the right hand side of (7) is the CRLB of $\boldsymbol{\theta}$. For the sinusoidal approximation considered here, a closed-form expression for the MCRLB of ω_0 may be found according to the following proposition.

Proposition 1. *The MCRLB for the pseudo-true frequency ω_0 corresponding to* (4) *when the observed signal is generated from* (1) *is given by*

$$\mathcal{M}(\omega_0) = \frac{\sigma^2}{\alpha^2} N\beta \frac{a_2^2 - (N-1)a_1 a_2 + a_1^2(N-1)(2N-1)/6}{2(a_1 a_3 - a_2^2)^2} \tag{10}$$

where

$$\beta = \left|\sum_{t=0}^{N-1} e^{-i\frac{r}{2}\left((N-1)t - t^2\right)}\right|^2$$

$$a_1 = \sum_{t=0}^{N-1}\eta_t \ , \ a_2 = \sum_{t=0}^{N-1} t\eta_t \ , \ a_3 = \sum_{t=0}^{N-1} t^2\eta_t,$$

with

$$\eta_t = \sum_{\tau=0}^{N-1} \cos\left(\frac{r}{2}\left((N-1)(t-\tau) - (t^2-\tau^2)\right)\right),$$

for $t = 0, 1, \ldots, N-1$. The proof of the proposition is summarized in the appendix. □

It is worth noting that in the case when $r = 0$, $\eta_t \equiv N$, and $\mathcal{M}(\omega_0)$ will be identical to the CRLB of a sinusoidal model. Furthermore, we note that $\mathcal{M}(\omega_0)$ provides a lower bound on the variance for estimates of ω_0. We are herein interested in the expected performance of the localization estimates, i.e., in the MSEs for estimates of φ_{N-1} and $\psi_{N-1} = g(\varphi_{N-1})$. With $\mathcal{M}(\omega_0)$ denoting the MCRLB, the MSEs may be readily computed as

$$\begin{aligned} MSE_{\varphi_{N-1}} &\triangleq \mathbb{E}_{p_x}\left((\varphi_{N-1} - \hat{\omega}_0)^2\right) \\ &= \mathcal{M}(\omega_0) + (\varphi_{N-1} - \omega_0)^2 \\ &= \mathcal{M}(\omega_0) + \left(\frac{r(N-1)}{2}\right)^2 \end{aligned}$$

and

$$\begin{aligned} MSE_{\psi_{N-1}} &\triangleq \mathbb{E}_{p_x}\left((\psi_{N-1} - g(\hat{\omega}_0))^2\right) \\ &= \left(\frac{\partial g(\omega)}{\partial \omega}\Big|_{\omega=\omega_0}\right)^2 \mathcal{M}(\omega_0) + (\psi_{N-1} - g(\omega_0))^2. \end{aligned}$$

Thus, letting $\mathcal{C}(\varphi_{N-1})$ denote the CRLB of φ_{N-1}, the sinusoidal approximation yields better location estimates than the chirp model if

$$MSE_{\psi_{N-1}} \leq \left(\frac{\partial g(\omega)}{\partial \omega}\Big|_{\omega=\varphi_{N-1}}\right)^2 \mathcal{C}(\varphi_{N-1}).$$

As we will illustrate in the numerical results, this inequality holds for a range of chirp rates. Also, in general,

$$\left(\frac{\partial g(\omega)}{\partial \omega}\Big|_{\omega=\omega_0}\right)^2 \mathcal{M}(\omega_0) \ll \left(\frac{\partial g(\omega)}{\partial \omega}\Big|_{\omega=\varphi_{N-1}}\right)^2 \mathcal{C}(\varphi_{N-1}),$$

i.e., the main limitation of using the sinusoidal approximation is the resulting squared bias.

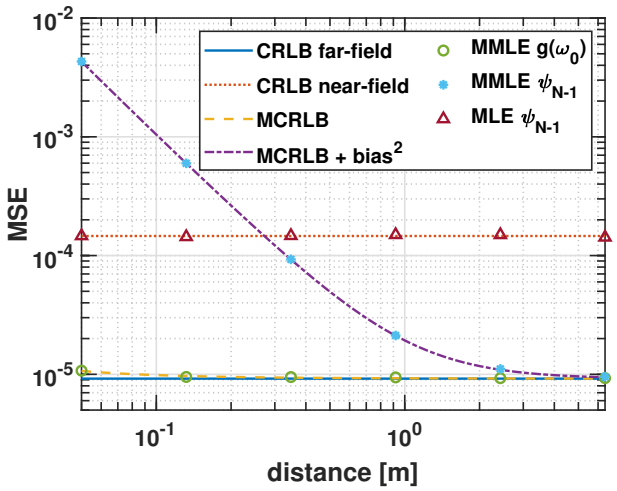

Fig. 2. Empirical estimator MSEs obtained from 10 000 Monte Carlo simulations, together with theoretical bounds and MSE, for fixed SNR 10 dB.

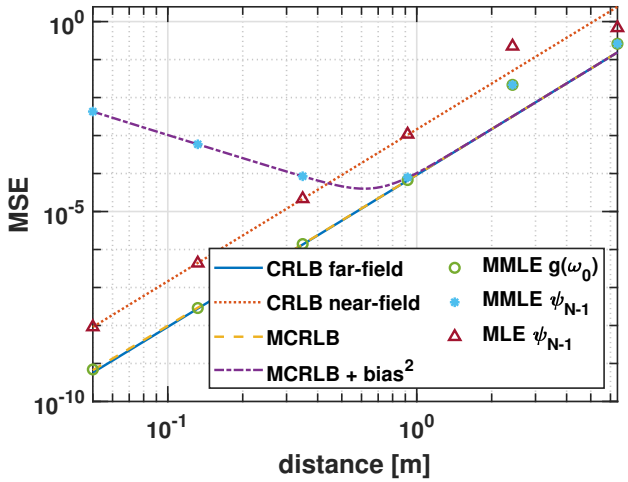

Fig. 3. Empirical estimator MSEs obtained from 10 000 Monte Carlo simulations, together with theoretical bounds and MSE, with SNR $\propto 1/d^4$.

IV. Numerical results

We proceed to illustrate the implications of the proposed model reduction in a simulation study using the localization setup in Figure 1. Specifically, we let the target angle be $\psi_{N-1} = \pi/4$, and study the MSE for the location estimate obtained from using the two alternative models, i.e., (1) and (4). The distance d to the target, is varied on the interval $[0.05, 6.4]$ m, i.e., the scenarios consider range from near-field to far-field, implying that the chirp rate decreases in absolute value as d increases. For each considered distance d, we perform 10 000 Monte Carlo simulations, in which the target angle is estimated based on the models in (1) and (4), where the signal parameter estimates are obtained using the MLE and MMLE, respectively. The parameters defining the setup in Figure 1 are the wavelength $\lambda = 5$ mm, the sampling frequency $f_s = 5700$ Hz, and the sensor movement speed is $v_0 = 0.2$ m/s.

Figure 2 shows the resulting CRLB for near- and far-field models, as compared with the MCRLB and the theoretical MSE for the misspecified model, here denoted MCRLB+bias^2, together with the MSE for both the correctly specified model, denoted MLE ψ_{N-1}, and the misspecified model, denoted MMLE ψ_{N-1}, as well as the variance of the misspecified estimator, denoted MMLE $g(\omega_0)$. In the case shown, we have, in order to illustrate how the distance to the target affects the achievable performance, fixed SNR $= 10$, with the SNR defined as SNR $= \alpha^2/\sigma^2$.

As may be seen in the figure, as the distance increases, the expected bias is reduced and the MCRLB approaches the far-field CRLB, indicating that using an estimator that assumes the sinusoidal model in (4) will yield preferable estimates than an estimator exploiting the signal's actual chirp model. It is worth noting that the difference between MCRLB and the far-field CRLB is very small even at relatively close range, meaning that the variance of using the sinusoid estimator will not become significantly worse even when the target is very close and the chirp rate is high. Instead, the dominant aspect reducing the performance of a sinusoidal estimator for high chirp rates will be the resulting bias, as is evident from the difference between MCRLB and MCRLB+bias^2. This bias is due to the sinusoid estimator finding the average frequency of a chirp, whereas the quantity of interest is actually the final frequency of the chirp. The most interesting point to note in Figure 2 is the intercept of the near-field CRLB and MCRLB+bias^2. For distances smaller than this point, the chirp model will yield a better estimate of the angle, whereas for distances larger than this point, the sinusoid model will yield a better estimate of the angle, assuming the SNR is constant at 10. In these simulations, the value for d was used in (3) to calculate the corresponding chirp rate r.

Figure 3 illustrates a more realistic situation, where the SNR varies with the distance between the transmitter and the target, d, such that the signal strength decreases proportionally to $1/d^4$. The main difference between the two simulations is thus that all the errors, as well as the bounds, increase as the distance grows as a result of the weakening signal strength. As can be seen in the figure, the MSE differs notably at larger distances, in spite of the large number of simulations; this effect is most likely due to the weak SNR, which also implies that the (asymptotic) bounds are no longer tight. The figure also shows that the chirp model will be preferable when the transmitter and target are closer than 0.44 m, and that the sinusoid model will be preferable when they are further apart.

Figure 4 displays the ratio of the theoretical MSE and CRLB corresponding to the models in (4) and (1), respectively, when varying the distance to the target as well as the power of the transmitted pulses. The signal strength is here expressed in terms of the SNR corresponding to a target distance of 1 m. As seen in the figure, the simplified model in (4) offers preferable performance for moderate to large distances, as well as in moderate to low SNR settings, despite being biased.

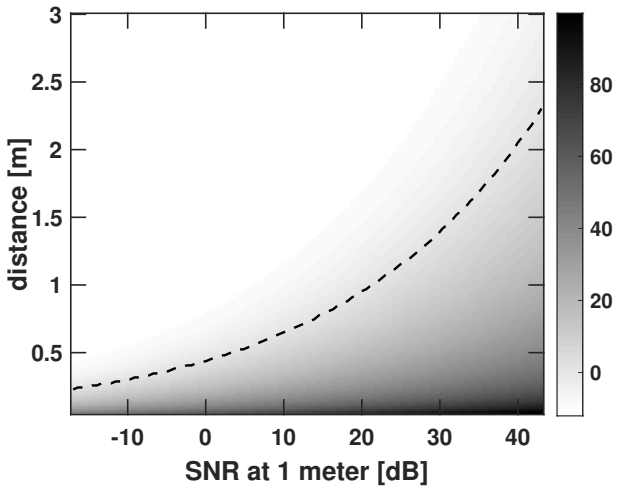

Fig. 4. Theoretical value of $10\log_{10}(MSE/CRLB)$ when varying the distance to the target, as well as the strength of the transmitted pulse. The dashed line marks the transition between the models, i.e., the model in (4) offers preferable performance above the line.

V. Conclusions

In this work, we have studied the implications of using simplified model structures for the close-range radar localization problem with a moving sensor system. Exploiting misspecified estimation theory, we derive an expression for the expected mean squared error of the angle to the target, being directly related to the distance to the target. This allows for determining which model should be employed for optimal estimation accuracy, depending on the measurement scenario, and, in particular, on the distance to the target.

Appendix

Expanding (8) and (9) under the assumption that p_x is a circularly symmetric white Gaussian distribution, it holds that

$$\begin{aligned}
A(\boldsymbol{\theta}_0) &= \mathbb{E}_{p_x}\left[\nabla^2_{\boldsymbol{\theta}} \ln p_\mu(\mathbf{y};\boldsymbol{\theta})\right]\Big|_{\boldsymbol{\theta}=\boldsymbol{\theta}_0} \\
&= \mathbb{E}_{p_x}\left[\nabla^2_{\boldsymbol{\theta}}\left(-\frac{1}{\sigma^2}\sum_t |y_t-\mu_t|^2\right)\right]\Big|_{\boldsymbol{\theta}=\boldsymbol{\theta}_0} \\
&= \mathbb{E}_{p_x}\left[\sum_t -\frac{2}{\sigma^2}\Re\left\{\frac{\partial \mu_t}{\partial \boldsymbol{\theta}}\frac{\partial \mu_t^*}{\partial \boldsymbol{\theta}} + (\mu_t - y_t)^*\nabla^2_{\boldsymbol{\theta}}\mu_t\right\}\right] \\
&= -\frac{2}{\tilde{\sigma}^2}\begin{bmatrix} N & 0 & 0 \\ 0 & \sum_t \Re\{\mu_t^* x_t\} & \sum_t \Re\{t\mu_t^* x_t\} \\ 0 & \sum_t \Re\{t\mu_t^* x_t\} & \sum_t \Re\{t^2\mu_t^* x_t\}\end{bmatrix}
\end{aligned}$$

and

$$\begin{aligned}
F(\boldsymbol{\theta}_0) &= \mathbb{E}_{p_x}\left[\nabla_{\boldsymbol{\theta}} \ln p_\mu(\mathbf{y};\boldsymbol{\theta})\nabla_{\boldsymbol{\theta}} \ln p_\mu(\mathbf{y};\boldsymbol{\theta})^T\right]\Big|_{\boldsymbol{\theta}=\boldsymbol{\theta}_0} \\
&= \frac{2\sigma^2}{\tilde{\sigma}^4}\sum_t \Re\{\nabla_{\boldsymbol{\theta}}\mu_t \nabla_{\boldsymbol{\theta}}\mu_t^*\} \\
&= \frac{2\sigma^2}{\tilde{\sigma}^4}\begin{bmatrix} N & 0 & 0 \\ 0 & Nr_0^2 & \frac{N(N-1)}{2}r_0^2 \\ 0 & \frac{N(N-1)}{2}r_0^2 & \frac{N(N-1)(2N-1)}{6}r_0^2\end{bmatrix},
\end{aligned}$$

where

$$\tilde{\sigma}^2 = \sigma^2 + \frac{1}{N}\sum_{t=0}^{N-1}|x_t - \mu_t|^2$$

is the pseudo-true misspecified noise variance. The MCRLB of ω_0 is given by the (3,3) element of $A(\boldsymbol{\theta}_0)^{-1}F(\boldsymbol{\theta}_0)A(\boldsymbol{\theta}_0)^{-1}$, yielding the result in (10).

References

[1] R. Watson-Watt, "Radar in war and peace," *Nature*, vol. 156, pp. 319–324, 1945.

[2] N. Levanon, *Radar Principles*, John Wiley & Sons, 1988.

[3] B. Edde, *Radar: Principles, Technology, Applications*, Prentice-Hall, Upper Saddle River, N.J., 1993.

[4] H. L. Van Trees, *Detection, Estimation, and Modulation Theory: Radar-Sonar Signal Processing and Gaussian Signals in Noise*, Krieger Publishing Co., Inc., 1992.

[5] A. L. Swindlehurst and P. Stoica, "Maximum likelihood methods in radar array signal processing," *Proc. IEEE*, vol. 86, no. 2, pp. 421–441, February 1998.

[6] A. Jakobsson, F. Gini, and F. Lombardini, "Robust Estimation of Radar Reflectivities in Multibaseline InSAR," *IEEE Trans. Aerosp. Electron. Syst.*, vol. 41, no. 2, pp. 751–758, 2005.

[7] N. Malesević, C. F. Wang, K. Rich, and C. Antfolk, "Fall prevention for elderly people using radar sensor: Feasibility study," *Resna Annual Conference 2019*, 2019.

[8] D. Montgomery, G. Holmén, P. Almers, and A. Jakobsson, "Surface classification with millimeter-wave radar using temporal features and machine learning," *Proc. of the 16th European Radar Conference*, 2019.

[9] H. S. Yeo and A. Quigley, "Radar sensing in human-computer interaction," *interactions*, vol. 25, pp. 70–73, 12 2017.

[10] J. Lien, N. Gillian, M. Karagozler, P. Amihood, C. Schwesig, E. Olson, H. Raja, and I. Poupyrev, "Soli: Ubiquitous gesture sensing with millimeter wave radar," *ACM Transactions on Graphics*, vol. 35, pp. 1–19, 07 2016.

[11] T. Kishigami, K. Kobayashi, M. Otani, T. Morita, H. Mukai, A. Saito, and Y. Nakagawa, "Advanced millimeter-wave radar system using coded pulse compression and adaptive array for pedestrian detection," in *2013 IEEE Radar Conference (RadarCon13)*, April 2013, pp. 1–6.

[12] P. Djurić and S. Kay, "Parameter Estimation of Chirp Signals," *IEEE Transactions on Acoustics Speech and Signal Processing*, vol. 38, pp. 2118–2126, 1990.

[13] X. Xia, "Discrete Chirp-Fourier Transform and Its Application to Chirp Rate Estimation," *IEEE Transactions on Signal Processing*, vol. 48, pp. 3122–3133, 2000.

[14] P. Stoica and R. Moses, *Spectral Analysis of Signals*, Prentice Hall, Upper Saddle River, N.J., 2005.

[15] H. White, "Maximum Likelihood Estimation Under Misspecified Models," *Econometrica*, vol. 50, no. 1, pp. 1–25, January 1982.

[16] C. D. Richmond and L. L. Horowitz, "Parameter Bounds on Estimation Accuracy Under Model Misspecification," *IEEE Trans. Signal. Process*, vol. 63, no. 9, pp. 2263–2278, 2015.

[17] S. Fortunati, F. Gini, M. S. Greco, and C. D. Richmond, "Performance bounds for parameter estimation under misspecified models: Fundamental findings and applications," *IEEE Signal Processing Mag.*, vol. 34, no. 6, pp. 142–157, Nov 2017.

[18] A. Mennad, S. Fortunati, M. N.-El Korso, A. Younsi, A. M. Zoubir, and A. Renaux, "Slepian-bangs-type formulas and the related Misspecified Cramér-Rao Bounds for Complex Elliptically Symmetric distributions," *Signal Process.*, vol. 142, pp. 320–329, Jan. 2018.

[19] F. Elvander, J. Ding, and A. Jakobsson, "On Harmonic Approximations of Inharmonic Signals," in *45th International Conference on Acoustic, Speech, and Signal Processing*, May 2020.

[20] P. Wang, T. Koike-Akino, M. Pajovic, P. V. Orlik, W. Tsujita, and F. Gini, "Misspecified CRB on parameter estimation for a coupled mixture of polynomial phase and sinusoidal fm signals," in *44th International Conference on Acoustic, Speech, and Signal Processing*, 5 2019, pp. 5302–5306.